Obtaining K and D meson properties from lattice QCD

Candidate number: 8301X
Supervisor: Dr. B. Chakraborty

May 2021

Abstract

Quantum Chromodynamics (QCD) describes the strong force and is an integral component of the Standard Model (SM). At low energies QCD cannot be solved perturbatively, however it is possible to find solutions by coarse-graining and computing on a lattice. Throughout this project, a Highly Improved Stagged Quark (HISQ) action is used. From statistical ensembles of 2-point correlators we are able to attempt to extract properties of particles such as the mass and partial decay width of mesons, using the well-known `corrfitter` and `lsqfit` Python packages. These properties depend both on a lattice discretisation error, and on the (unphysical) light quark mass of the HISQ action. Extrapolation to the chiral/contiuum limit is also performed in order to obtain properties that are physical. In particular, these techniques are well suited to work with stranged and charmed mesons on a $N_f = 2 + 1 + 1$ quark sea. The mass of mesons calculated here $m_{K^0} = 495.2(12), m_{D^0} = 1875.6(90)$ is consistent with results in literature, although the decay width extrapolation was unsuccessful.

Declaration: Except where specific reference is made to the work of others, this work is original and has not been already submitted either wholly or in part to satisfy any degree requirement at this or any other university.

Contents

1 Introduction **3**
- 1.1 Standard Model . . . 3
- 1.2 Quantum Chromodynamics . . . 3
- 1.3 Lattice QCD . . . 4
- 1.4 Fermion Doubling . . . 4
- 1.5 Highly Improved Staggered Quark Action . . . 5
- 1.6 Correlators . . . 5

2 Statistical Methods and Data **6**
- 2.1 Data . . . 6
- 2.2 Jacknife Averaging . . . 6
- 2.3 χ^2 Fitting . . . 7
- 2.4 Bayesian Analysis . . . 7
- 2.5 Project Development . . . 7

3 Preliminary study **8**

4 Data Analysis **9**
- 4.1 Fit convergence . . . 10
- 4.2 Results . . . 10

5 Chiral-Continuum Extrapolation **14**
- 5.1 Mass . . . 14
- 5.2 Partial Decay Width . . . 15

6 Conclusion **16**
- 6.1 Results . . . 16
- 6.2 Further Work . . . 16

1 Introduction

1.1 Standard Model

The Standard Model is currently the most accurate model of particle physics. It describes fermions: quarks (q), leptons (l), and their antiparticles, denoted with an overline ($\overline{q}$). It also describes the gauge bosons which mediate the strong, weak, and electromagnetic (EM) fields.

There are 6 flavours of quarks, in 3 different generations. Quarks are coupled to the strong, weak, and EM interactions. The leptons, also in 3 generations, are coupled to the EM field if they are charged, and to the weak force. In this project, we are extracting the mass and decay widths of $K^0 = s\overline{d}$ and $D^0 = c\overline{u}$ neutral mesons[1]. Due to the very short range being studied, with a total area of interest having side length $L \approx 5\,\text{fm}$, the strong force completely dominates. As a result, the weak and EM interactions can be completely neglected in the action, leaving only the strong interaction which is governed by the theory of Quantum Chromodynamics (QCD).

1.2 Quantum Chromodynamics

QCD is a $SU(3)$ gauge field theory governing the interactions of quarks and gluons. As quarks are fermions, they are described by a Dirac lagrangian coupled to an external gauge field. For a quark field annihilation operator ψ_f, Dirac field creation operator $\overline{\psi} = \psi_f^\dagger \gamma^0$ with quark flavour f, we have[1, 2]:

$$\mathcal{L} = \sum_f \psi_f^\dagger (i \not{D} - m_f)\psi_f - \frac{1}{4} F^a_{\mu\nu} F_a^{\mu\nu} \tag{1}$$

In this Lagrangian we have a gauge covariant derivative $\not{D} = \not{\partial} + i g_s \not{A}^a \lambda_a / 2$[2]. Here and in the rest of this section, we leave the indices referring to colour implicit. However to be clear, the quarks carry a conserved *colour charge* analogous to the electric charge in QED. There are three separate *colours* which are often called *red*, *green*, and *blue*[3]. The colour of a quark is represented by a colour spinor, which is the space acted on by the matrix λ_a. It is these indices, referring to the matrix multiplication, that are omitted.

The other important quantity is the gluon field strength tensor:

$$F^a_{\mu\nu} = \partial_\mu A^a_\nu - \partial_\nu A^a_\mu - g_s f_{abc} A^b_\mu A^c_\nu \tag{2}$$

Here the latin indices label the 8 generators[4] ($t_a = \lambda_a/2$) of the QCD $\mathfrak{su}(3)$ Lie algebra with (totally antisymmetric) structure constants $[t_a, t_c] = i f_{abc} t_c$. These generators are considered to be linearly independent colour charges of gluons. A^a_μ are the respective 4-potentials, which are coupled to the quarks.

[1] Or equivalently, their antiparticles.

[2] Using Feynman slash notation so that for any 4-vector $\not{B} = B_\mu \gamma^\mu$, where the γ form a representation of the spinor group that acts on fermions.

[3] Although, the choice of basis is arbitrary and can be transformed by any matrix $U \in SU(3)$.

[4] λ_a are the Gell-Mann matrices, which form a basis of $SU(3)$.

Unlike in QED, QCD allows for self-interaction of the gauge bosons. As a result, QCD is known as an asymptotically-free theory: as interactions are taken to higher energies, the forces involved become weaker. This leads to colour confinement, where only bound states with zero overall colour charge can be isolated. Traditional perturbation theory expands a system at low energy, but in the case of QCD this would give divergent forces which would invalidate such a method. Instead, a common approach is solving systems on a lattice.

1.3 Lattice QCD

Lattice QCD is a method to solve QCD systems by placing the fields on a spacetime lattice. To see how this is done we first consider the path integral formulation of QFT. To compute the expectation of an operator, we take a functional integral of the Lagrangian over all possible field configurations[3, 2]

$$\langle \mathcal{O} \rangle = \frac{1}{\mathcal{Z}} \int \mathcal{D}\psi \, \mathcal{O} \exp\left(i \int \mathrm{d}^4 x \, \mathcal{L}(\psi, \partial\psi) \right), \tag{3}$$

$$\mathcal{Z} = \int \mathcal{D}\psi \quad \exp\left(i \int \mathrm{d}^4 x \, \mathcal{L}(\psi, \partial\psi) \right), \tag{4}$$

where $\mathcal{Z}$ is the partition function. This is named in analogy with the statistical partition function, which can be obtained by performing a Wick rotation $t \mapsto it$.

Clearly it is not usually feasible to integrate over an infinite-dimensional space of functions, so we use a technique called regularisation. To do this we replace the $4D$ continuum integral by a spacetime lattice. Often an isotropic lattice is chosen (with lattice spacing a), which is the case in this project.

We define the quark fields[2] $\psi(x)$ only on lattice points x_μ, and the gluon fields $U_{\hat{\delta}}(x) = U(x, x + \hat{\delta})$ defined on the links between the lattice points. The links are specified as written, by a point x^μ and a unit vector $\hat{\delta}^\mu$ specifying the direction along the lattice. The conjugate field $U^\dagger_{\hat{\delta}}(x) = U(x + \hat{\delta}, x)$ gives the link from $x + \hat{\delta}$ back to x. Once we have our particle fields, it is possible to replace derivatives with differences in fields at adjacent lattice sites. One can then construct an appropriate gauge invariant action, called the Wilson action.

We hope that by using this lattice model of QCD, we can produce sensible results in the limit of a short lattice spacing. Unfortunately, when the computations are carried out there are a lot of discretisation errors[4]. By a careful choice of discrete derivative and by using the Highly Improved Staggered Quark (HISQ) action, we can remove $\mathcal{O}(a)$ error terms. This leaves us with a discretised theory with errors in $\mathcal{O}(a^2)$, which we hope is small enough that our extrapolation to $a \to 0$ is accurate.

1.4 Fermion Doubling

In Equation 1, the term $M = i\not{D} - m_f$ can be considered the inverse quark propagator, and many important calculations depend on the propagator M^{-1}. When fermions are placed on a finite lattice, this inverse propagator takes the form in Equation 5[5]. This is periodic in p_μ, which gives rise to the phenomenon of fermion doubling.

In each of the 3+1 dimensions there is an extra *taste* of fermion at the end of the Brillouin zone. This corresponds to a total of $16 = 2^4$ tastes. The physical taste is the fermion with the smallest p, and is thus the ground state. Lattice operators can be constructed to interact with any of these tastes. For example, Goldstone tastes use a local $\gamma^5 = i\gamma^0\gamma^1\gamma^2\gamma^3$ operator. Alternatively, non-Goldstone fermions can be chosen by using a non-local, or point-split, γ^5 operator. In any case, the splitting between tastes is a function of the lattice spacing, and so in the continuum limit the physical property is restored.

$$M^{-1} = \frac{-i\gamma^\mu \sin(ap_\mu)/a + m}{\sin(ap^\mu)\sin(ap_\mu)/a^2 + m^2} \tag{5}$$

1.5 Highly Improved Staggered Quark Action

It can be beneficial to reduce the number (or impact) of these extra fermion tastes. Two of these methods are outlined here. The first uses Wilson quarks[5], where an extra term is introduced into the Lagrangian, such that the unphysical tastes are given non-zero mass in the continuum limit, which decouples them from the theory. Unfortunately, this explicitly breaks chiral symmetry.

The alternative, and the one used to generate all the data used for this project, is the Highly Improved Staggered Quark (HISQ) action. Here, Highly Improved refers to the removal of $\mathcal{O}(a)$ discretisation terms. By spin-diagonalising the naive fermion action, it is possible to reduce the number of doublers to 4, which is more computationaly efficient.

1.6 Correlators

All the results in this project come directly from the 2-point correlator (Equation 6) where $\overline{\phi}$ is the field creation operator for the meson of interest. Our state $|0\rangle$ is populated with a randomised background gluon configuration.

$$G^{2pt}(x_0, x) = \langle 0|\, \phi(x)\overline{\phi(x_0)}\, |0\rangle \tag{6}$$

Naively, we expect[5] to see a 2-point correlator $G^{2pt}(\overrightarrow{p}; t) = \sum_n a_n^2 \exp(-E_n t)$. However due to the periodic boundary conditions, there is an additional term where $t \to T - t$ for T the time length of the lattice. A further complication comes from oscillation terms. Recall that we are using a staggered quark action, where we still have 4 fermion doublers. In each of the 3+1 dimensions, the formalism gives an additional term proportional to $(-1)^{\hat{\delta}^\mu}$. For the 3 spatial dimensions, this is averaged out over adjacent sites, but in the time dimension this does not happen so we are left with an oscillatory term. This gives our final expression for the 2-point correlator,

$$G(t) = \sum_n a_n^2(e^{-E_n t} + e^{-E_n(T-t)}) + (-1)^t \sum_n a_{on}^2(e^{-E_{on} t} + e^{-E_{on}(T-t)}). \tag{7}$$

One thing to note is that these oscillatory terms are due to opposite parity states. That is, if we are studying a $K^0 = d\overline{s}$, the additional term comes from the $\overline{K^0} = s\overline{d}$

Label	a (fm)	$N_t \times N_x^3$	m_l/m_s	$n_{\text{cfg}} \times n_{\text{c}}$	β	w_0/a	$am_l^{\text{sea/val}}$	am_s^{sea}	am_c^{sea}	am_s^{val}	am_c^{val}	Z_{disc}
Very Coarse	0.1509	48×32^3	0.036	998×16	5.8	1.1367(5)	0.002 35	0.0647	0.831	0.0678	0.8605	0.991 97
Coarse	0.124 04	64×24^3	0.2	1053×16	6.0	1.3826(11)	0.0102	0.0509	0.635	0.0656	0.664	0.996 83
Fine	0.090 23	96×32^3	0.2	499×16	6.3	1.9006(20)	0.0074	0.037	0.440	0.0376	0.449	0.998 92

Table 1: Parameters of various datasets used throughout this project. We take the Wilson flow parameter $w_0 = 0.1715(9)\,\text{fm}$[7]. Valence quarks are directly interacted with, such as being the components of mesons that we are studying. The sea quarks are virtual particles that create the background for each configuration.

state[5]. As a result this term does not appear for a meson composed of exactly one type of quark, eg. $\pi^0 = u\overline{u}$ or $d\overline{d}$.

2 Statistical Methods and Data

2.1 Data

The data for this project has been produced by using relativistic HISQ action for both valuence and sea quarks on publicly available gauge configurations generated by MILC collaboration[6]. The configurations have sea quark effects from up/down (light), strange, and charm quarks ($N_f = 2 + 1 + 1$). The specific datasets that have been used are given in Table 1.

By using a finite lattice we have discretisation errors (discussed in Section 1.3), which we can only eliminate by extrapolating from multiple datasets, to the contiuum limit. Additionally, for computational reasons it is not possible to use physical light quark masses for all lattice sizes. As a result, we must also extrapolate to the chiral limit, where $m_l = 0$, which is close to the physical value of $m_l \approx 0.02 m_s$.

2.2 Jacknife Averaging

Given a large sample of data with completely unknown errors, we often want to compute unbiased estimators for statistical parameters. One such way is to use Jacknife averaging[8]. Consider a sample of n i.i.d. values $x_i \sim F$. Construct n mean estimates $\overline{x}_i = \sum_{j \neq i} \frac{x_j}{n-1}$. The average of these sample means $\overline{x} = \sum_i \frac{\overline{x}_i}{n}$ is precisely the mean of the whole sample, and the error on this estimate is given by the variance $\text{Var}[\overline{x}] = \frac{n-1}{n} \sum_i (\overline{x}_i - \overline{x})^2$ of the distribution of $\overline{x}_i$. That is, we have an unbiased estimator for the mean and standard defiation of F given by $\overline{x} \pm \sqrt{\text{Var}[\overline{x}]}$. In fact by replacing the means $\overline{x}_i$ above by (almost) any estimator $\overline{\theta}_i$, it is possible to construct an new estimator, using a slightly more laborious method, which has an asymptotically smaller bias[9].

[5]This is the only instance where we are careful to distinguish a neutral meson from its antiparticle.

2.3 χ^2 Fitting

A common technique for fitting a model to data is to minimise the statistic

$$\chi^2 = \sum_n (y_n - f(x_n))^2/\sigma_n, \tag{8}$$

where y_n is the observed value with error σ_n at a point x_n, and f depends on the model parameters. Varying the parameters and then recomputing the χ^2 statistic allows us to find the maximum-likelihood values. This is the method in the Python software packages `lsqfit` and by extension `corrfitter`[10][6]. The procedure is performed until the statistic reaches a stable minimum.

For a general χ^2 fit, there are N data points and P parameters, where we take the degrees of freedom[7] $K = N - P$. The statistic should follow a χ^2_K distribution. As a result, the reduced statistic $\chi^2/K \lesssim 1$ indicates a good quality fit. It is also import to take care with small reduced χ^2 results, as extremely small values might be indicative of an overfit.

2.4 Bayesian Analysis

Using the `corrfitter`[12] Python package, we perform a least-squares regression on our 2-point correlator (Equation 7) data (Jacknife averages of results characterised in Table 1). For a given set of priors and a data set, the least-squares regression gives best-fit values for parameters of choice. In the context of this project, we are interested in fitting the amplitudes a_n, a_{on} and the log of the energy differences, $\log(\mathrm{d}E_n)$, $\log(\mathrm{d}E_{on})$. In particular, the log of energy differences allows us to implicitly force the energy levels of the fit to strictly increase.

2.5 Project Development

This project originally had the title "Tuning NRQCD b-quarks for Bottomonium spectroscopy using lattice QCD". For that project, I would have taken existing code to generate correlator data using lattice Non-Relativistic QCD (NRQCD) and modified it. To use NRQCD for b-quark mesons, the modification would have been to use *an*isotropic lattices. In particular, using a finer lattice spacing in the time dimension would have helped to keep discretisation errors small, while keeping computations relatively fast by leaving the spatial lattice spacing at a coarser scale.

Due to the time constraints of a project of this nature, it was decided that it was not possible to tackle such an intricate problem. There was instead a pivot towards the final title of this project. This is much more focussed on the data-analysis side, exploring modern techniques for obtaining masses and partial decay widths of lighter[8] mesons.

[6] Technically this works on a similar but more accurate statistic, where the errors are given as a matrix, due to the correlated nature of errors coming from the Jacknife average.

[7] For a sufficiently well behaved function f, see[11].

[8] Not containing b-quarks.

3 Preliminary study

Using Jacknife averaging on the fine dataset (recall that these have $T = 96$ time slices) was analysed. Here we have data for K and D mesons in the physical taste, and an additional non-Goldstone D taste, which we expect to have a slightly higher mass. For the D meson sets there are 489 gauge configurations, and 495 for the K meson.

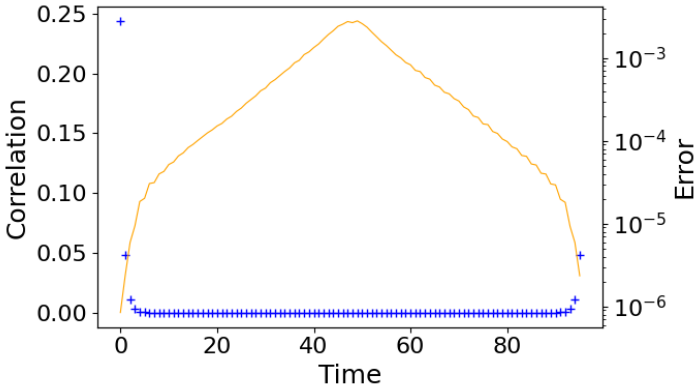

Figure 1(a): In blue, the average correlator for Goldstone D meson on a fine lattice. In orange, the (statistical) relative error.

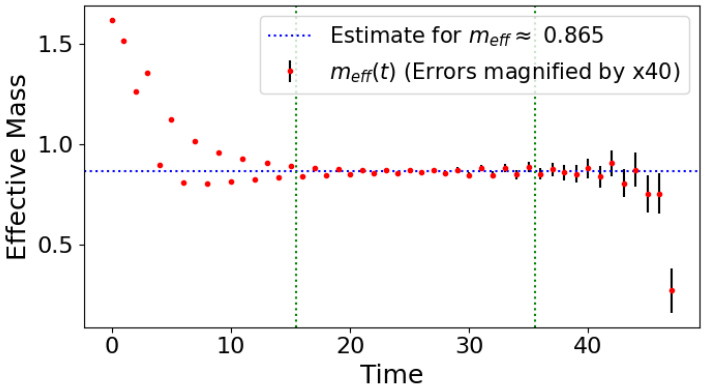

Figure 1(b): Estimate for m_{eff} for Goldstone D meson on a fine lattice. Only points between the green lines are included in the final average.

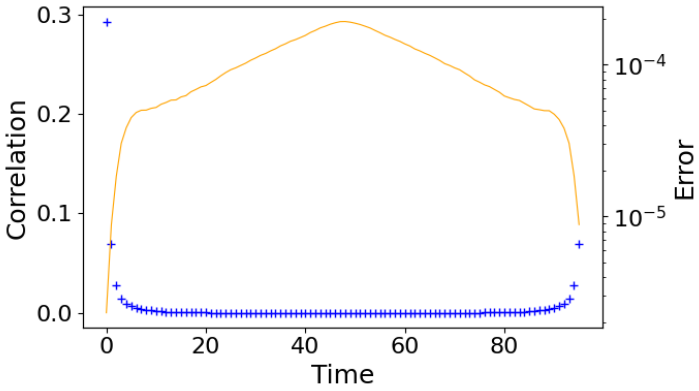

Figure 2(a): In blue, the average correlator for K meson on a fine lattice. In orange, the (statistical) relative error.

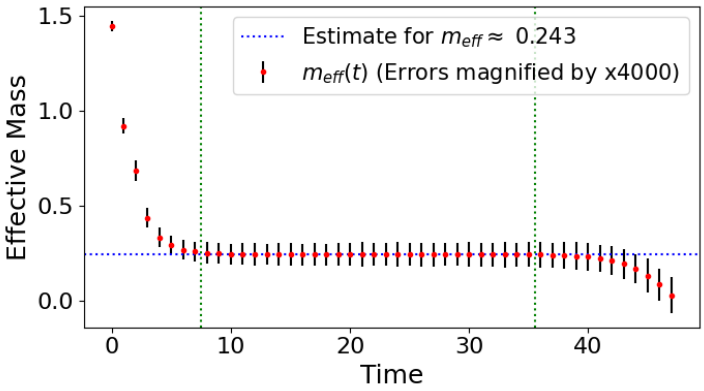

Figure 2(b): Estimate for m_{eff} for K meson on a fine lattice. Only points between the green lines are included in the final average.

If we assume the oscillatory terms are small then one can look near the middle of the data. Looking at Figures 1a, 2a, 3a it is clear to see that the correlators have in fact plateaud at this point. Here the only relevant term is the ground state (a_0, E_0) as all higher energy levels have decayed faster. As a result, in this region we should be able to compute an estimate for the ground state effective mass,

$$m_{\text{eff}}(t) = \log\left(\frac{G(t)}{G(t+1)}\right). \tag{9}$$

When actually computing this value, we must make sure that we do not go past halfway through the data, as the second half (with rising exponentials) will lead to a

Meson	m_{eff} (lattice units)	m_{eff} (MeV)
K	0.243	531
D Goldstone	0.865	1891
D non-Gold	0.866	1894

Table 2: Effective mass results for all 3 datasets on a fine lattice. These values are unstable to changing the averaging region, so they should only be taken as a rough estimate.

negative effective mass albeit with the same magnitude. Additionally it is helpful to avoid the areas with larger errors. We can see that for both of the physical tastes, we have a good region where the effective mass has reached a plateau, and for the non-Goldstone D meson the region is still not too bad. To find an estimate for the overall m_{eff} we average within this whole region, although the choices of endpoints are somewhat ad-hoc. It should be noted that for both of the D meson tastes, there are sufficient oscillations that moving the ends of the region can cause either taste to appear more massive. It seems that the effective mass calculation is insuffient to distinguish the staggered quark tastes at the fine lattice spacing.

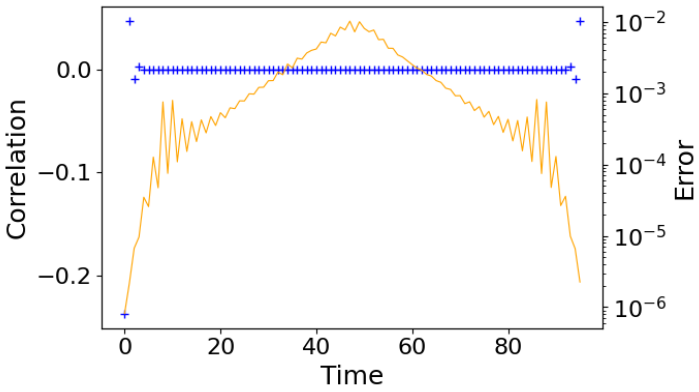

Figure 3(a): In blue, the average correlator for a non-Goldstone D meson on a fine lattice. In orange, the (statistical) relative error.

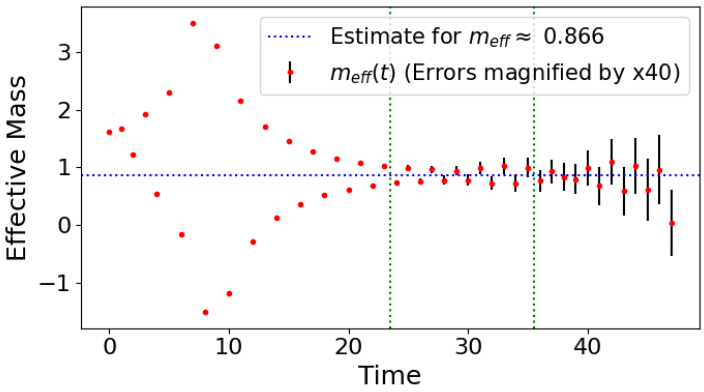

Figure 3(b): Estimate for m_{eff} for non-Goldstone D meson on a fine lattice. Only points between the green lines are included in the final average.

4 Data Analysis

Throughout this section, all correlator data has been Jackknife averaged to give an estimated Gaussian variable at each time slice. The analysis code is a very heavily modified version of code provided by Chakraborty, which includes optimised prior values. Throughout this analysis we are fitting up to 6 terms in the correlator (Equation 7). It is not reasonable to extract physical results from most of these terms, however we can certainly look at the ground state of each meson. Taking the most reliable value of meson mass for each of the data sets, it is possible to extrapolate to the chiral and contiuum limits to compute final estimates for the neutral K and D meson masses.

During the analysis, there are two main fitting parameters that are varied. t_{min} tells the fitting software how many time slices to ignore from the start and the end of each

set of correlator data. This is useful as there are extra effects happening at these early time scales, and we would like to ignore these for simplicity. The other parameter, n, corresponds to the number of exponentials for which we are providing prior data. Studying energy levels larger than n is completely unreasonable as these are only used to acheive a better fit, and the values are unphysical.

For all datasets that are analysed, we limit the fitting for K mesons to only have $t_{\min} = 3$. For D mesons we vary this as $t_{\min} \in \{3, 4, 5, 6, 7, 9\}$. For both mesons, we also vary $n \in \{1, \ldots, 6\}$. In all of the following plots, $n = 4$ was determined to be the most reliable point, so all values given on the plots are evaluated here. For plots showing fitting results, error bars are indicated in red. When a data point (error bar) appears missing it is either too large (small) to be shown on the scale. For convenience, the first 4 data points of the fitting quality plots have also been reproduced on the plots, as the majority of these points are far too large to be shown on the same scale as the rest of the points.

4.1 Fit convergence

The fine dataset corresponds to a lattice spacing $a \approx 0.09\,\text{fm}$ and a light quark mass $m_l \approx 0.2m_s$. For the K meson, it is clear that for any value of $n \geq 4$, the fit has converged (Figure 4[9]). Inspection of the results for D meson show that the fits tend to converge first for $n = 3$ or 4. Now we turn to the fit quality, where as we can see in Figure 5, the fitting converged well for all $t_{\min}$ and for all $n \geq 4$.

The coarse dataset corresponds to a lattice spacing $a \approx 0.12\,\text{fm}$ and a light quark mass $m_l \approx 0.2m_s$. In this dataset, we can see that the K meson values (Figure 6) actually converge for $n = 3$. More generally, the fit quality (Figure 7) suggests that $n = 3$ or 4 are the earliest parameters that converge, although this is more reliable for higher $t_{\min}$.

The very coarse dataset corresponds to a lattice spacing $a \approx 0.15\,\text{fm}$ and a light quark mass $m_l \approx 0.036m_s$. Here we see that the K meson fit (Figure 8) apepars to converge even for $n = 2$. The fit quality plots (Figure 9) show a different result however. Even at higher $t_{\min}$, the χ^2 parameter does not reach a reasonable value until at least $n = 3$.

4.2 Results

Taking into account the values of parameters for which all the datasets had reliable fits, the smallest (and least likely to lead to overfitting) viable choices for the parameters are $n = 4$ and $t_{\min} = 6$. The collection of E_0 and a_0 values that are found with these parameters is given in Table 3. The energy values here seem reasonable as they correspond roughly to the masses provided in[13]: $m_K \approx 498\,\text{MeV}$ and $m_D \approx 1865\,\text{MeV}$. Of course, these values are far outside the provided statistical error bounds, but this is expected as we have both unphysical quark masses, and discretisation errors. Our next step will extrapolate our values to the chiral-continuum limit, which should give accurate results.

[9]Plots of this form have been produced for all combinations of dataset and $t_{\min}$, however where they do not add to the discussion, they have been ommitted.

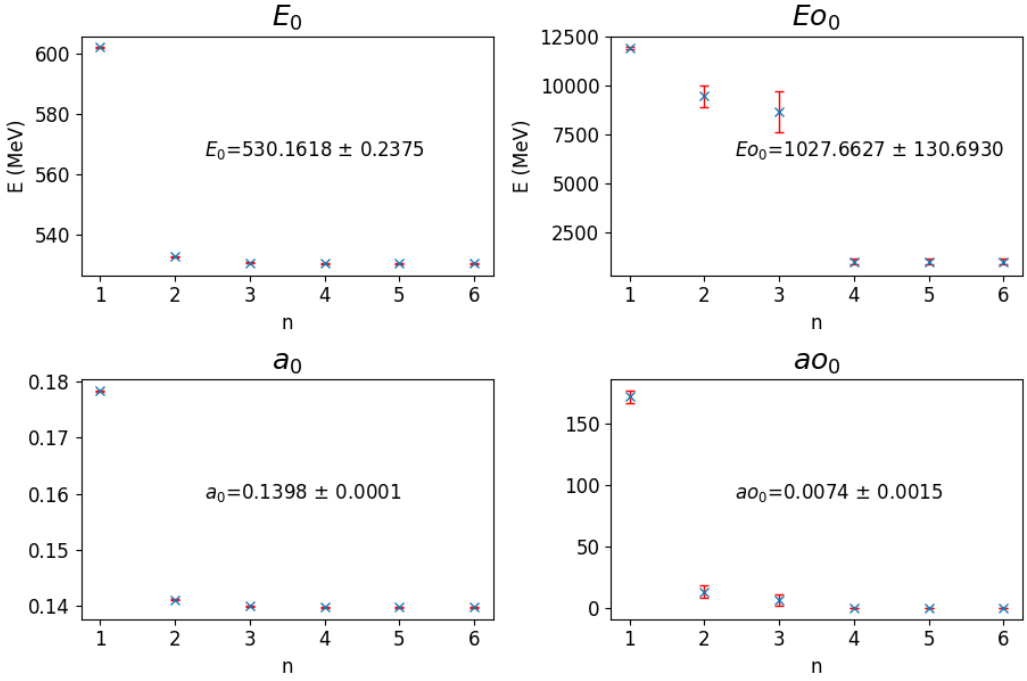

Figure 4: K meson fitting results on a fine lattice.

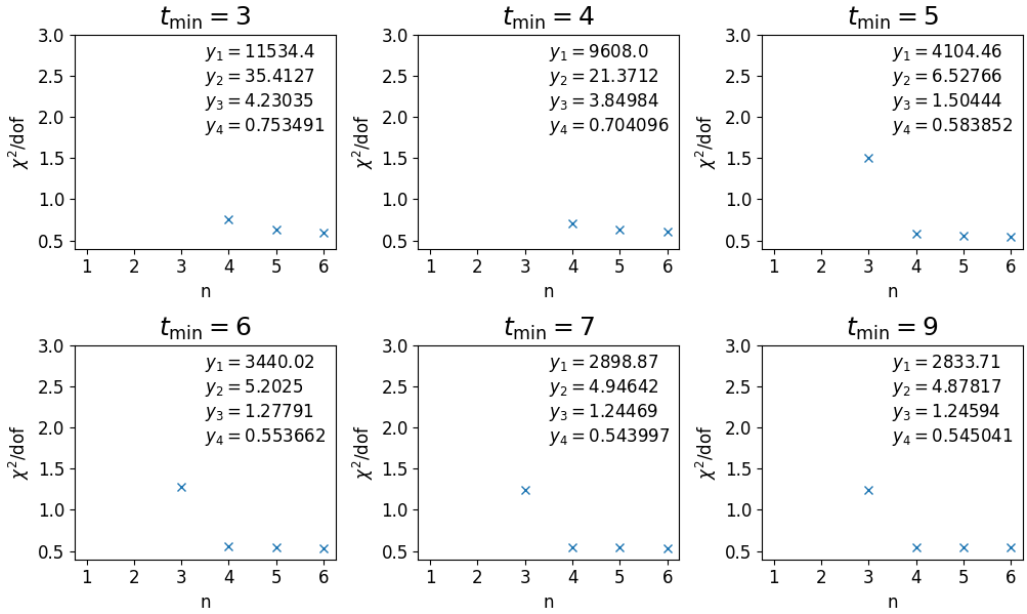

Figure 5: Fitting quality for fine lattice.

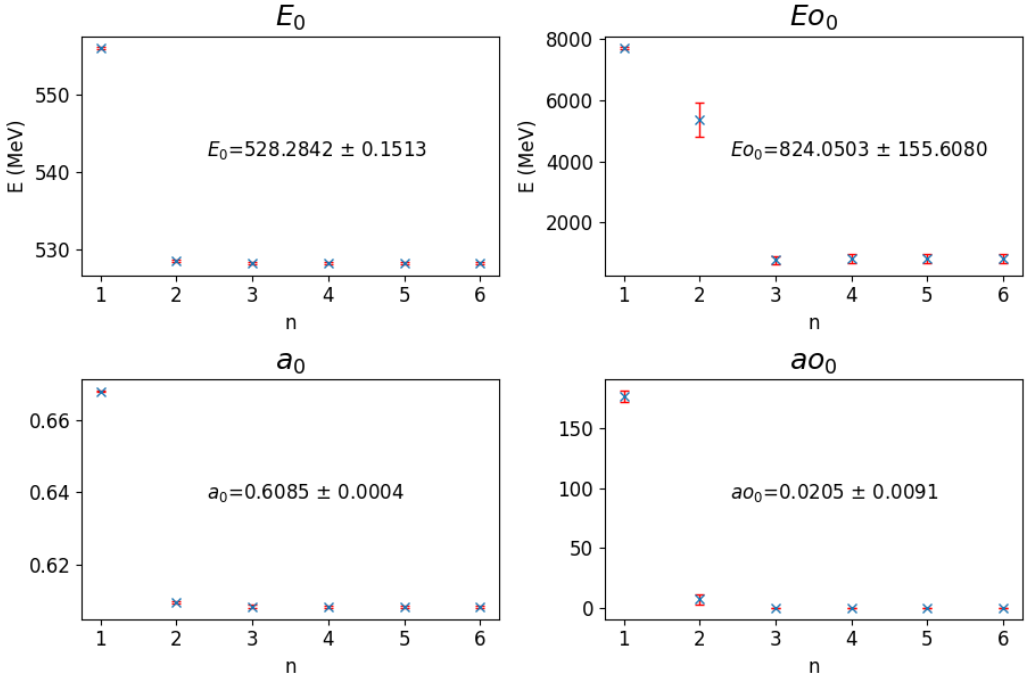

Figure 6: K meson fitting results on a coarse lattice.

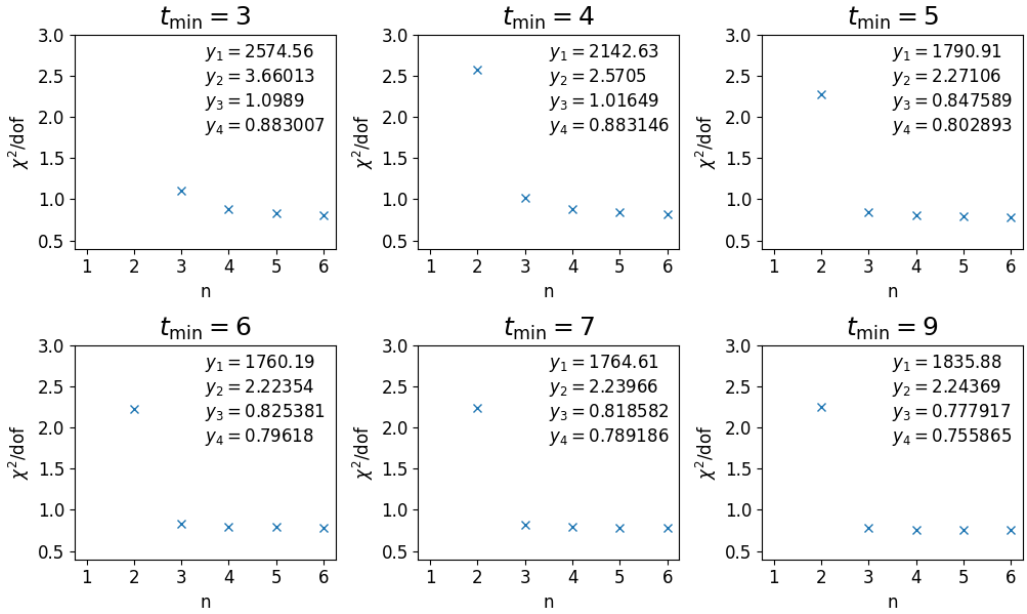

Figure 7: Fitting quality for coarse lattice.

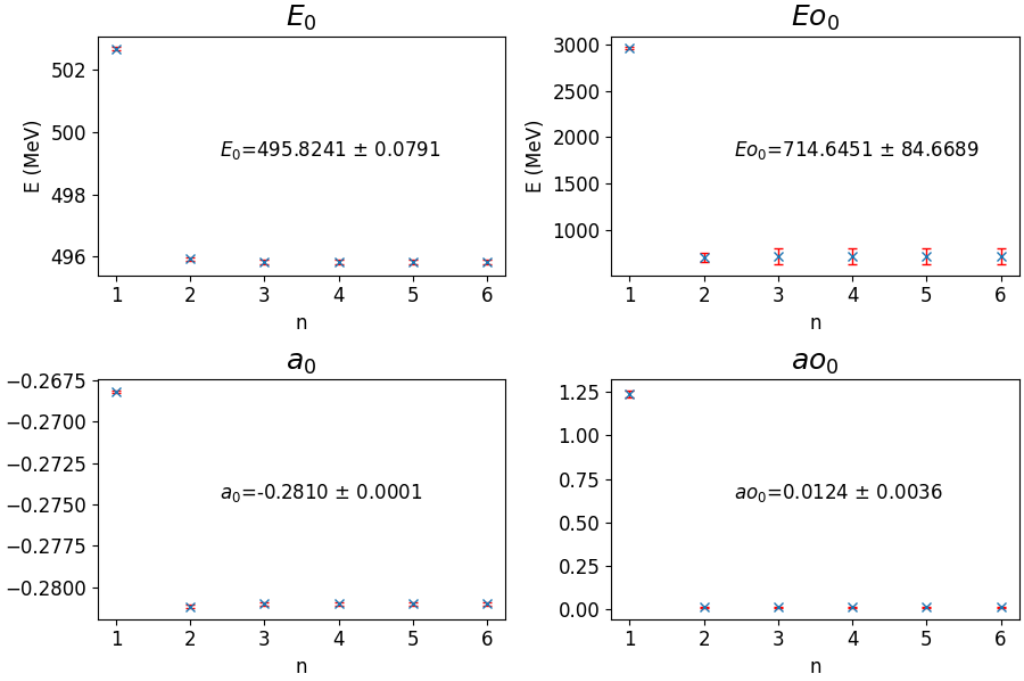

Figure 8: K meson fitting results on a very coarse lattice.

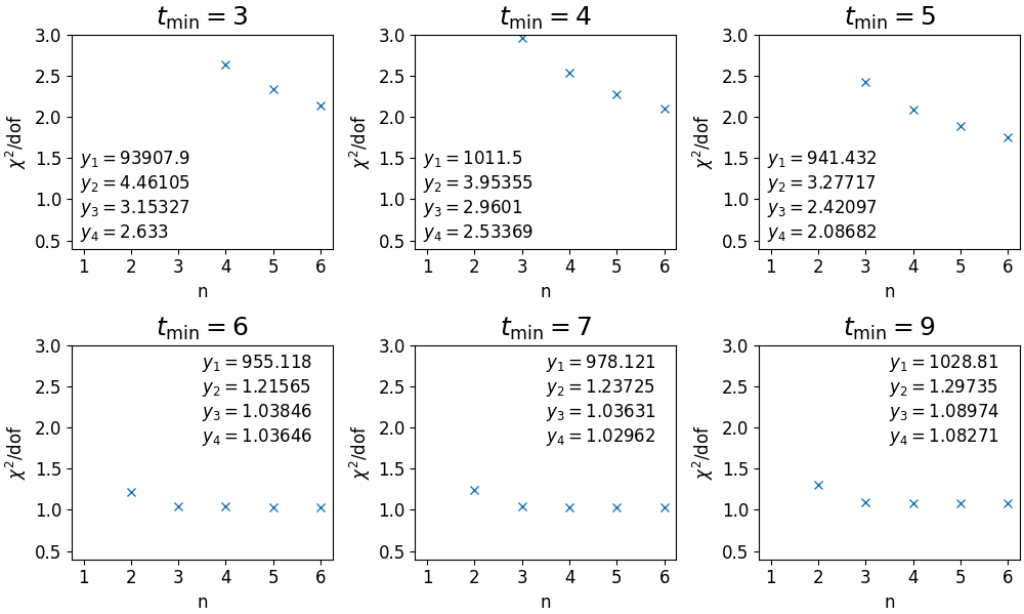

Figure 9: Fitting quality for very coarse lattice.

			E_0 (MeV)		$\lvert a_0\rvert$	
Label	a (fm)	m_l/m_s	K	D	K	D
Very Coarse	0.15	0.036	495.92(08)	1887.3(51)	0.281 01(11)	0.2286(65)
Coarse	0.12	0.2	528.28(15)	1893.0(15)	0.608 53(37)	0.1880(12)
Fine	0.09	0.2	530.16(24)	1889.3(11)	0.139 78(12)	0.1242(07)

Table 3: Results from fitting all datasets. $t_{\text{min}} = 6$ for D mesons, and $n = 4$ for all results. Uncertainties given in parentheses are statistical.

	E_0 (MeV)		Predicted E_0 (MeV)	
Label	K	D	K	D
Very Coarse	495.92(08)	1887.3(51)	495.92(08)	1887.3(51)
Coarse	528.28(15)	1893.0(15)	528.31(25)	1892.8(15)
Fine	530.16(24)	1889.3(11)	530.13(24)	1889.4(11)
Chiral/Continuum limit	-	-	495.2(12)	1874.6(90)

Table 4: Comparison of observed and predicted (via Equation 10) mass values, including the extrapolated chiral/continuum limit values.

5 Chiral-Continuum Extrapolation

5.1 Mass

Using the results we found above, it should be possible to extrapolate down to the chiral (physical light quark mass) and continuum (to avoid discretisation errors) limits. From Equation 16 in [14] we know that we should be able to model this extrapolation well. However, we have a total of 6 values that we are fitting, so it would be dubious to fit a model with any more than 6 parameters. As a result, we take the 3 lowest order terms (each produces a pair of parameters for K and D mesons respectively) which gives us

$$m = m_{\text{phys}} \left(1 + 5c_\delta \frac{m_l}{m_s} + c_{a^2}(a\Lambda)^2\right). \tag{10}$$

In this, the factor of 5 is to convert to chiral scale, and the factor of $\Lambda = 500\,\text{MeV}$ sets the appropriate energy scale and non-dimensionalises c_{a^2}. When we perform a χ^2 fit to these values[10] we find a $\chi^2/\text{dof} = 0.29$ which signifies a good quality fit. This also does not appear to be overfit, which was a concern given that we are fitting 6 parameters to 6 data points. Table 4 shows that the predicted values match very well with the observed values, as expected. Also shown are the extrapolated values which are consistent with results from the literature[13], $m_{K^0} = 497.611(13)\,\text{MeV}$ and $m_{D^0} = 1864.83(5)\,\text{MeV}$ to within 3σ of our statistical uncertainty. These are all shown together in Figure 10.

[10]The priors used for this fit are advised by the same source.

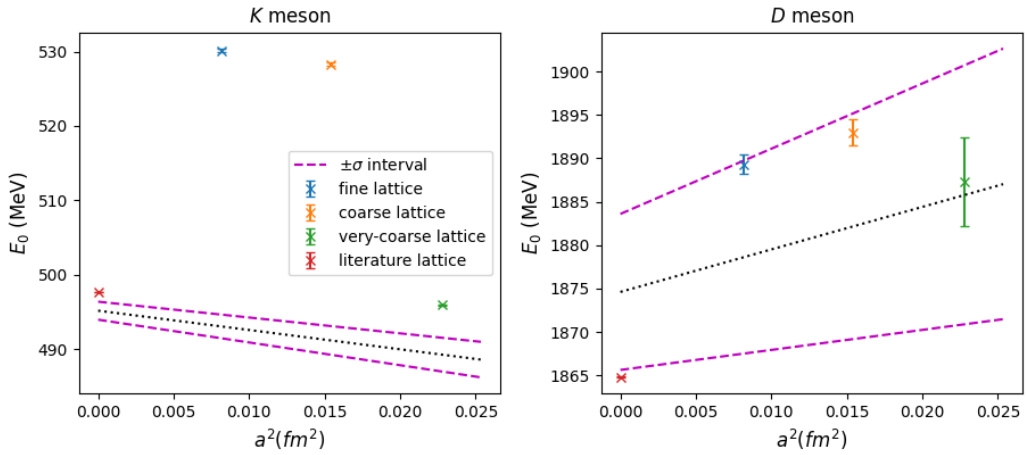

Figure 10: At $m_l/m_s = 0$, the bands show the variation of E_0 with a^2. Recall that each of the lattice values use non-zero light quark mass, so we do not expect fine and coarse lattice values to be within these bands. The very coarse lattice value has the smaller quark mass so is expected to be closer to the chiral limit, which is exactly what we see here. Where error bars are not clearly shown, they are too small to be visible.

5.2 Partial Decay Width

From [14] it is possible to write the normalised decay constant of a meson M as

$$f_M = (m_q + m_{\bar{q}})a_0\sqrt{\frac{2}{E_0^3}}, \tag{11}$$

where a_0 and E_0 are the ground state amplitude and energy respectively for a dataset. We can also write the partial decay width as

$$\Gamma(M) = \frac{4\pi}{3}\alpha_{QED}^2 e_q^2 \frac{f_M^2}{m_M}, \tag{12}$$

where $\alpha_{QED} \approx \frac{1}{137}$ at this scale, $e_q = \frac{1}{3}$ is the charge in units of e. We expect the physical decay width to take the same dependence on a and $\frac{m_l}{m_s}$ as m in Equation 10. By running the same chiral-continuum extrapolation we should obtain a decay constant for each meson, which may be converted to a partial decay width. Unfortunately, with just these data points, given in Table 5 and shown in Figure 11, it was not possible to compute a successful fit. For completeness, the $\chi^2/\text{dof} \approx 37 \gg 1$, so the fit completely failed. With more data points it may be possible to diagnose the cause of this, however with just the 3 (varying in 2 parameters) that have been studied here, this is not viable in this case.

Label	f_K	f_D
Very Coarse	0.003 467 1(16)	0.005 02(14)
Coarse	0.007 910(7)	0.004 160(27)
Fine	0.001 677 9(19)	0.002 756(26)

Table 5: Normalised decay constants for each lattice and meson type.

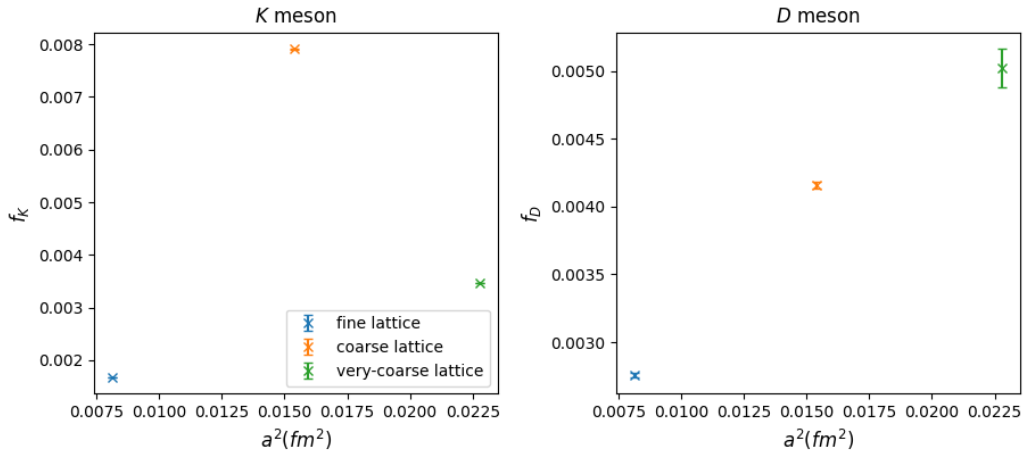

Figure 11: The variation of f_M with a^2 as calculated via Equation 11. Again note that these data points do not necessarily use the same light quark masses. Where error bars are not clearly shown, they are too small to be visible.

6 Conclusion

6.1 Results

This project has been primarily focussed on data analysis. The first part was important as a first step to check that data was in fact of the form that we expected. Indeed we found that for a specific set of HISQ parameters, $m_{D^0}^{\text{eff}} \approx 1900\,\text{MeV}$. This approximation only involved fitting the first (i.e. ground state) exponential and no oscillatory terms, but still gave a result within around 5 % of what was expected.

The second part constituted the majority of the effort of the project. Here, 3 datasets with varying light quark mass and lattice spacing were analysed using an existing tool. This gave far more precise values for both the mass and amplitudes of the mesons, presented in Table 3. Again we saw that the meson masses were consistent with expected results, except with this data we were also able to notice the variation with respect to the HISQ parameters.

Finally, with a selection of meson masses, it was possible to extrapolate to the chiral/continuum limit. The aim here was to find physical meson masses and partial decay widths. Table 4 shows the extrapolated masses, which were within 3σ of the literature values. A prediction of the partial decay widths was also planned, however no successful fit was found.

6.2 Further Work

This project followed existing techniques in lattice NRQCD so the next steps have already been explored well. The key advances to make would likely include adding more datasets. That is, a larger variety of light quark masses, and lattice spacings. By increasing the number of datasets analysed it would become viable to fit more parameters to Equation 10. This could give a tighter fit and thus reduce the statistical error on the final results. With careful enough analysis it is possible to also calculate masses, amplitudes,

and decay widths for excited states. Among these generalisations, more parameters may also help to find a valid fit for the decay constants of mesons. Alternatively, considering extra tastes may add insightful contributions to these extrapolations.

References

[1] G. Shaw F. Mandl. *Quantum Field Theory*. John Wiley & Sons, 2010.

[2] Brian Colquhoun. "Bottomonium and B Physics with Lattice NRQCD b Quarks". University of Glasgow, 2015.

[3] R. P. Feynman. "Space-Time Approach to Non-Relativistic Quantum Mechanics". In: *Rev. Mod. Phys.* 20 (2 Apr. 1948), pp. 367–387. DOI: 10.1103/RevModPhys.20.367.

[4] Christof Gattringer and Christian B Lang. *Quantum Chromodynamics on the Lattice: An Introductory Presentation*. eng. Vol. 788. Lecture notes in physics. Berlin, Heidelberg: Springer Berlin / Heidelberg, 2009. ISBN: 3642018491.

[5] Bipasha Chakraborty. "Precision tests of the standard model using lattice QCD". University of Glasgow, 2016.

[6] A Bazavov et al. "Lattice QCD ensembles with four flavors of highly improved staggered quarks". In: *Physical Review D* 87.5 (2013), p. 054505.

[7] RJ Dowdall et al. "V u s from π and K decay constants in full lattice QCD with physical u, d, s, and c quarks". In: *Physical Review D* 88.7 (2013), p. 074504.

[8] Bradley Efron. *The jackknife, the bootstrap and other resampling plans*. SIAM, 1982.

[9] Avery McIntosh. "The Jackknife estimation method". In: *arXiv preprint arXiv:1606.00497* (2016).

[10] G Peter Lepage et al. "Constrained curve fitting". In: *arXiv preprint hep-lat/0110175* (2001).

[11] Rene Andrae, Tim Schulze-Hartung, and Peter Melchior. "Dos and don'ts of reduced chi-squared". In: *arXiv preprint arXiv:1012.3754* (2010).

[12] G Peter Lepage. *corrfitter*. Version 8.1.1. 2020. URL: https://github.com/gplepage/corrfitter.

[13] Particle Data Group et al. "Review of Particle Physics". In: *Progress of Theoretical and Experimental Physics* 2020.8 (Aug. 2020). 083C01. ISSN: 2050-3911. DOI: 10.1093/ptep/ptaa104. eprint: https://academic.oup.com/ptep/article-pdf/2020/8/083C01/34673740/rpp2020-vol2-2015-2092_18.pdf. URL: https://doi.org/10.1093/ptep/ptaa104.

[14] Bipasha Chakraborty et al. "Nonperturbative comparison of clover and HISQ quarks in lattice QCD and the properties of the phi meson". In: *arXiv preprint arXiv:1703.05552* (2017).